

DOI: 10.1002/cphc.201100652

# Domain-Specific Folding Kinetics of Staphylococcal Nuclease Observed through Single-Molecule FRET in a Microfluidic Mixer\*\*

Zeyong Zhi,<sup>[a]</sup> Pengcheng Liu,<sup>[a, b]</sup> Peng Wang,<sup>[a]</sup> Yanyi Huang,<sup>[c]</sup> and Xin Sheng Zhao\*<sup>[a]</sup>

Characterization of the free-energy landscape in protein folding is key to understanding the “folding code” contained in the sequence.<sup>[1]</sup> Multidomain proteins represent a predominant fraction of the whole proteome in prokaryotic and—even more—in eukaryotic cells.<sup>[2]</sup> It is thus interesting to find out how these multidomain proteins fold. A number of multidomain proteins have been shown to fold with multistate kinetics before the native population appears,<sup>[3]</sup> and the information is usually extracted from elaborate modeling.<sup>[4]</sup> It would be nice if one could directly probe the heterogeneous populations of unfolded and folded ensembles along the folding pathway from the initial denatured state to the final native conformation.

Single-molecule fluorescence resonance energy transfer (smFRET) offers a powerful tool to probe the heterogeneous system of protein molecules.<sup>[5]</sup> Meanwhile, microfluidic laminar-flow mixers have facilitated kinetic measurements of biological systems by ultrafast mixing.<sup>[6]</sup> The combination of smFRET and a kinetic microfluidic mixer was first introduced by Lipman et al. in 2003 to rapidly trigger protein folding and to reveal the evolution of folded and unfolded species under non-equilibrium conditions.<sup>[7]</sup> Since then, this method has been developed to achieve a shorter mixing time,<sup>[8]</sup> and the shortest record of 0.2 ms was reported very recently.<sup>[9]</sup> Other types of microfluidic devices, such as a coaxial 3D mixer<sup>[10]</sup> and a mixer with enhanced photostability,<sup>[11]</sup> have also been proposed. The combined smFRET and microfluidic mixing technique has been applied to the protein folding inside the GroEL<sup>[12]</sup> and the folding of an intrinsically disordered protein.<sup>[9]</sup> Staphylococcal nuclease (SNase), consisting of an N-terminal  $\beta$ -sheet domain and a C-terminal  $\alpha$ -helical domain, has been studied as a model for multidomain protein folding and exhib-

ited a complex kinetic behavior.<sup>[4,13]</sup> Our previous equilibrium smFRET studies have shown that a domain-specific collapse occurs in the early stages of the refolding process.<sup>[13c]</sup>

Herein, we report our non-equilibrium smFRET studies in a microfluidic mixer to directly probe the transition rate from the unfolded state to the native folded state after the collapse. We labeled donor and acceptor dyes at selected sites to detect the kinetics of the conformational reorganization of the subdomains and the global molecule in the refolding landscape. By examining the unfolded and folded states, the kinetic measurements suggested that different domains adopt different searching pathways to reach the native conformation.

We constructed three mutants K28C/K97C, K97C/K136C, and K28C/H124C (Figure 1A) and labeled them with fluorescent dyes using the same procedure reported previously.<sup>[13c]</sup> The mutants were site-directed labeled with thiol-reactive fluores-

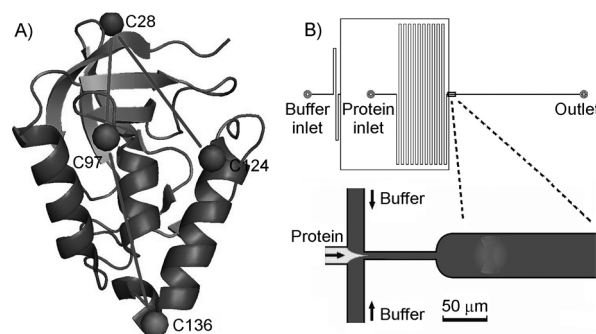


**Figure 1.** Labeling scheme on SNase and schematics of the microfluidic mixer. A) Mutants for the folding kinetic measurements: K28C/K97C spans the  $\beta$ -sheet domain, K97C/K136C spans the  $\alpha$ -helical domain, and K28C/H124C spans the two domains. B) Schematics of the microfluidic mixer. The denaturant was rapidly diluted in the neck region, where the protein also accomplishes the initial collapse. Then, the unfolded protein initiates its folding in the detection channel.

cence dyes of Alexa Fluor 546 and Alexa Fluor 647. A more detailed description of the mutation and labeling process is given in the Supporting Information. The mutant of K28C/K97C was designed to probe the  $\beta$ -sheet domain. K97C/K136C was for the  $\alpha$ -helical domain. Finally, the mutant of K28C/H124C was constructed to probe the conformational change of the whole molecule while maintaining a sensitive distance comparing to the Förster radius,  $R_0$ , between the donor–acceptor dye pair. The structure, the stability, and the enzymatic activity of the mutants K28C/K97C and K28C/H124C have been characterized already.<sup>[13c]</sup> We verified K97C/K136C using far-UV circular dichroism (CD) spectroscopy (Figure S1 of the Support-

[a] Dr. Z. Zhi, Dr. P. Liu, P. Wang, Prof. Dr. X. S. Zhao  
Beijing National Laboratory for Molecular Sciences  
State Key Laboratory for Structural Chemistry  
of Unstable and Stable Species, Department of Chemical Biology  
College of Chemistry and Molecular Engineering  
and Bio-dynamic Optical Imaging Center  
Peking University, Beijing 100871 (P. R. China)  
Fax: (+86) 10-62751708  
E-mail: zhaoxs@pku.edu.cn

[b] Dr. P. Liu  
National Key Laboratory of Biomacromolecules  
Institute of Biophysics, CAS, Beijing 100101 (P. R. China)

[c] Prof. Dr. Y. Huang  
College of Engineering, and Biodynamic Optical Imaging Center,  
Peking University, Beijing 100871 (P. R. China)

[\*\*] FRET: Fluorescence Resonance Energy Transfer

Supporting information for this article is available on the WWW under <http://dx.doi.org/10.1002/cphc.201100652>.

ing Information) and the denaturation curves using the intrinsic fluorescence of Trp 140. The thermodynamic parameters were derived from the denaturation curves and are shown in Table S1 of the Supporting Information. Both results demonstrated that the K97C/K136C mutant kept the native structure well.

A microfluidic mixer was constructed (Figure 1B) following the essential ideas proposed by Pfeil et al.<sup>[8]</sup> and Lemke et al.,<sup>[11]</sup> with minor modifications to fit our need and capacity of microfabrication. The details and the characterization of the mixer have been described previously<sup>[14]</sup> (see also the Supporting Information). The major consideration of the design was to maintain a stable laminar flow for an optimal smFRET measurement with high photon bursts (maximum bursts of 80–100) and good signal-to-noise ratio (~100). The microfluidic mixer was aligned on a confocal microscope by an adaptor. The protein sample and the buffer were delivered into the inlets from two reservoirs, which were connected to compressed air. The mixing time of the microfluidic device was characterized to be 0.15 s<sup>[14]</sup> by the extremely fast process of protein collapse, suitable for current kinetic measurements. During the mixing time, the SNase molecule collapses with a very fast rate, while the transition from the unfolded to the folded state barely occurs.<sup>[14]</sup> The velocities at the detection points were measured by fluorescence correlation spectroscopy (FCS), simultaneously with the smFRET data acquisition, to calculate the definite time versus the position.<sup>[9,14]</sup> The labeled protein was in the unfolded state in 2 M GdmCl and was injected into the central inlet. The native buffer was delivered through the two side inlets which were originated from an entrance. The concentration of the labeled protein was less than 60  $\mu\text{M}$  in the detection channel by comparing the event-counting frequency with equilibrium experiments. The denaturant concentration was 0.49 M in the detection channel, which was determined by comparing the FRET efficiency of the unfolded state with that in the equilibrium experiments (see the Supporting Information). 1  $\mu\text{M}$  unlabeled wild-type SNase purified by desalting column was added into both lines to prevent protein adhesion.

The setup for the smFRET measurements was essentially identical to that reported previously (see also the Supporting Information).<sup>[13c]</sup> The residence time of the protein molecule in the laser focus was on the order of 1 ms. As individual labeled protein molecules flowed through the laser focus, which was 10  $\mu\text{m}$  above the coverglass in the detection channel, fluorescent photons from the donor and acceptor were counted separately by two avalanche photodiode (APD) detectors and the histograms of FRET efficiency were generated, with each histogram consisting of at least 3000 identified events at an appro-

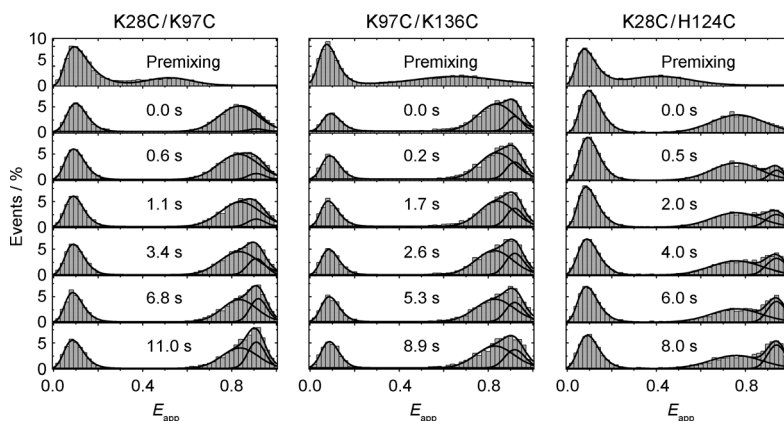


**Figure 2.** FRET efficiency histograms (at various times) for the mutants. The top panel shows the unfolded state in the central channel before mixing. The time zero was taken at the conjunction of the neck and the detection regions.

priate threshold (the sum of the photon counts from the donor and acceptor channels) to pick up the signal bursts. By scanning the laser focus along the central line of the detection channel, the kinetic evolution of the FRET efficiency distribution after the mixing was mapped (Figure 2).

The initial protein collapse was extremely fast. The time resolution of our microfluidic mixer was limited by the mixing process and was unable to probe the rate of the collapse.<sup>[15]</sup> During the mixing in the neck region, the shift of the peak of the unfolded state was the result of the protein collapse from a loose form to a more compact form.<sup>[14]</sup> In the detection channel, we observed the growth of the peak associated with the native state as well as the decrease of the population of the unfolded molecules. Finally, the FRET efficiency histogram approached its equilibrium under the given GdmCl concentration. The unfolded and folded states were fitted using the Gaussian function and lognormal function, respectively.<sup>[5a,b]</sup> We also fitted the folded states using a beta function<sup>[13c,16]</sup> and found that both functions delivered identical results within the experimental error. The peak near zero was the background generated from molecules without active acceptor or impurities in solution.<sup>[17]</sup> The peak of the subpopulations in the FRET efficiencies remained constant, indicating that the mean end-to-end distances of the donor and acceptor in both unfolded and folded states did not change during the folding reaction. This observation showed that single-molecule kinetic measurements can resolve the unfolded and folded species so that it excluded the complexity encountered in an ensemble experiment.<sup>[4]</sup>

SNase has been shown to fold through the pathway of multiple intermediate states using the ensemble stopped-flow method by tracking the Trp fluorescence.<sup>[4,13a]</sup> In our case, the data of a single domain could be well fitted using a single-exponential curve, while a double-exponential curve was needed to satisfactorily fit the data of the whole molecule (see Figure 3 and Figure S4 of the Supporting Information). For the  $\beta$ -sheet mutant of K28C/K97C, the fitting yielded a folding relaxation lifetime of  $\tau = 4.5 \pm 0.8$  s. For the  $\alpha$ -helical domain of

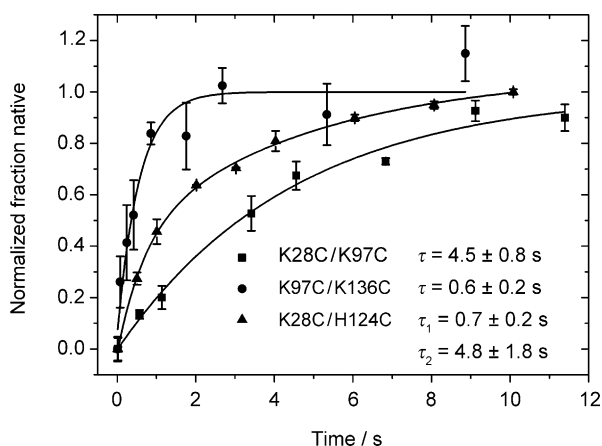


**Figure 3.** Single-molecule folding kinetics of the different subdomains and the whole molecule.

K97C/K136C, the fitted lifetime was  $\tau = 0.6 \pm 0.2$  s. Modeling the folding of the global molecule of K28C/H124C generated lifetimes of  $\tau_1 = 0.7 \pm 0.2$  s and  $\tau_2 = 4.8 \pm 1.8$  s, corresponding to the lifetimes of the single-domain mutants well. Our observed folding lifetimes were comparable to the folding kinetics measured by ensemble CD spectra.<sup>[18]</sup> Here, our results could be assigned in a straightforward way: the  $\alpha$ -helical subdomain folds about ten times faster than the  $\beta$ -sheet subdomain. This result provided an alternative view from the previous CD study which says that the sheet-like chain conformations precede the main-chain folding reaction.<sup>[18]</sup> The subtle difference comes from the fact that the CD study mainly detects the changes of the secondary structure during the processes of collapse and folding, while the smFRET study mainly detects the distance between the residues under investigation. Another conventional tool in the protein-folding study is the tryptophan fluorescence, where the change of the tryptophan fluorescence reflects the variation of the microenvironment around the tryptophan residues instead of the whole domain.<sup>[4]</sup> It has been reported that proline isomerization occurs on the order of tens of seconds,<sup>[19]</sup> but we were unable to find such a process due to our short time window. The data sets gathered by using different tools represent different aspects of the complicated protein folding, and they are complementary to each other. The trait of the smFRET technique resides on its capability of directly identifying the unfolded and folded species and directly assigning the rate to a selected process by site-directed mutagenesis and dye labeling.

It was pointed out by Pfeil et al. that diffusion would erode the relationship between the reaction time and the position by the time on the order of  $t = a^2/2D$ , where  $a$  is the half width of the detection channel and  $D$  is the diffusion constant of the protein.<sup>[8]</sup> With  $D = 73 \mu\text{m}^2\text{s}^{-1}$  for the SNase molecule and  $a = 25 \mu\text{m}$  for our apparatus,  $t = 4.3$  s was derived. According to this rough criterion, our measured reaction-time constants could have a deviation from the true values. It is easy to argue that diffusion would make the observed reaction-time constant smaller than it should be, and the slower the reaction, the

bigger the deviation. Therefore, if the effect of diffusion were not negligible, the difference of the refolding times between the  $\alpha$ -helical and the  $\beta$ -sheet subdomains would be even bigger than what we observed.

In summary, we coupled smFRET and microfluidic mixing to directly explore the substructural folding kinetics of a protein with two subdomains after the initial collapse. Our conclusion is that the  $\alpha$ -helical subdomain of SNase folds faster than the  $\beta$ -sheet subdomain, so that the folding kinetics of SNase is subdomain-specific.

## Experimental Section

Further information on Methods, as well as Figures S1–S4 and Table S1, is available in the Supporting Information.

## Acknowledgements

The work was supported by NSFC (20733001, 20973015) and by NKBRF (2006CB910300, 2010CB912302).

**Keywords:** FRET • microfluidic mixer • proteins • single-molecule studies • SNase

- [1] a) A. R. Dinner, A. Sali, L. J. Smith, C. M. Dobson, M. Karplus, *Trends Biochem. Sci.* **2000**, *25*, 331–339; b) A. I. Bartlett, S. E. Radford, *Nat. Struct. Mol. Biol.* **2009**, *16*, 582–588.
- [2] J. Fitter, *Cell. Mol. Life Sci.* **2009**, *66*, 1672–1681.
- [3] a) S. E. Radford, C. M. Dobson, P. A. Evans, *Nature* **1992**, *358*, 302–307; b) R. L. Baldwin, G. D. Rose, *Trends Biochem. Sci.* **1999**, *24*, 77–83.
- [4] K. Maki, H. Cheng, D. A. Dolgikh, H. Roder, *J. Mol. Biol.* **2007**, *368*, 244–255.
- [5] a) B. Schuler, E. A. Lipman, W. A. Eaton, *Nature* **2002**, *419*, 743–747; b) A. Hoffmann, A. Kane, D. Nettels, D. E. Hertzog, P. Baumgartel, J. Lengefeld, G. Reichardt, D. A. Horsley, R. Seckler, O. Bakajin, B. Schuler, *Proc. Natl. Acad. Sci. USA* **2007**, *104*, 105–110; c) S. D. Pugh, C. Gell, D. A. Smith, S. E. Radford, D. J. Brockwell, *J. Mol. Biol.* **2010**, *398*, 132–145.
- [6] a) J. B. Knight, A. Vishwanath, J. P. Brody, R. H. Austin, *Phys. Rev. Lett.* **1998**, *80*, 3863–3866; b) D. E. Hertzog, B. Ivorra, B. Mohammadi, O. Bakajin, J. G. Santiago, *Anal. Chem.* **2006**, *78*, 4299–4306; c) L. J. Lapidus, S. Yao, K. S. McGarrity, D. E. Hertzog, E. Tubman, O. Bakajin, *Biophys. J.* **2007**, *93*, 218–224; d) H. Y. Park, S. A. Kim, J. Korlach, E. Rhoades, L. W. Kwok, W. R. Zipf, M. N. Waxham, W. W. Webb, L. Pollack, *Proc. Natl. Acad. Sci. USA* **2008**, *105*, 542–547.
- [7] E. A. Lipman, B. Schuler, O. Bakajin, W. A. Eaton, *Science* **2003**, *301*, 1233–1235.
- [8] S. H. Pfeil, C. E. Wickersham, A. Hoffmann, E. A. Lipman, *Rev. Sci. Instrum.* **2009**, *80*, 055105.
- [9] Y. Gambin, V. Vandelinder, A. C. Ferreol, E. A. Lemke, A. Groisman, A. A. Deniz, *Nat. Methods* **2011**, *8*, 239–241.
- [10] K. M. Hamadani, S. Weiss, *Biophys. J.* **2008**, *95*, 352–365.
- [11] E. A. Lemke, Y. Gambin, V. Vandelinder, E. M. Brustad, H.-W. Liu, P. G. Schultz, A. Groisman, A. A. Deniz, *J. Am. Chem. Soc.* **2009**, *131*, 13610–13612.
- [12] H. Hofmann, F. Hillger, S. H. Pfeil, A. Hoffmann, D. Streich, D. Haenni, D. Nettels, E. A. Lipman, B. Schuler, *Proc. Natl. Acad. Sci. USA* **2010**, *107*, 11793–11798.
- [13] a) W. F. Walkenhorst, S. M. Green, H. Roder, *Biochemistry* **1997**, *36*, 5795–5805; b) K. Maki, H. Cheng, D. A. Dolgikh, M. C. R. Shastry, H. Roder, *J. Mol. Biol.* **2004**, *338*, 383–400; c) P. C. Liu, X. L. Meng, P. Qu, X. S. Zhao, C. C. Wang, *J. Phys. Chem. B* **2009**, *113*, 12030–12036.
- [14] Z. Y. Zhi, P. C. Liu, Y. Y. Huang, X. S. Zhao, *Acta Phys. Chim. Sin.* **2011**, *27*, 1990–1995.

- [15] D. Nettels, I. V. Gopich, A. Hoffmann, B. Schuler, *Proc. Natl. Acad. Sci. USA* **2007**, *104*, 2655–2660.
- [16] M. Dahan, A. A. Deniz, T. Ha, D. S. Chemla, P. G. Schultz, S. Weiss, *Chem. Phys.* **1999**, *247*, 85–106.
- [17] K. A. Merchant, R. B. Best, J. M. Louis, I. V. Gopich, W. A. Eaton, *Proc. Natl. Acad. Sci. USA* **2007**, *104*, 1528–1533.
- [18] Z. D. Su, M. T. Arooz, H. M. Chen, C. J. Gross, T. Y. Tsong, *Proc. Natl. Acad. Sci. USA* **1996**, *93*, 2539–2544.
- [19] K. Maki, T. Ikura, T. Hayano, N. Takahashi, K. Kuwajima, *Biochemistry* **1999**, *38*, 2213–2223.

---

Received: August 24, 2011

Revised: October 17, 2011

Published online on November 16, 2011

---

# CHEMPHYSICHEM

## Supporting Information

© Copyright Wiley-VCH Verlag GmbH & Co. KGaA, 69451 Weinheim, 2011

### **Domain-Specific Folding Kinetics of Staphylococcal Nuclease Observed through Single-Molecule FRET in a Microfluidic Mixer\*\***

Zeyong Zhi,<sup>[a]</sup> Pengcheng Liu,<sup>[a, b]</sup> Peng Wang,<sup>[a]</sup> Yanyi Huang,<sup>[c]</sup> and Xin Sheng Zhao<sup>\*[a]</sup>

cphc\_201100652\_sm\_miscellaneous\_information.pdf

## SUPPORTING INFORMATION FOR

# Domain Specific Folding Kinetics of Staphylococcal Nuclease Observed through Single-Molecule FRET in Microfluidic Mixer

Zeyong Zhi<sup>1,3</sup>, Pengcheng Liu<sup>1,3</sup>, Peng Wang<sup>1,3</sup>, Yanyi Huang<sup>2,3</sup>, Xin Sheng Zhao<sup>1,3\*</sup>

<sup>1</sup>Beijing National Laboratory for Molecular Sciences, State Key Laboratory for Structural Chemistry of Unstable and Stable Species, Department of Chemical Biology, College of Chemistry and Molecular Engineering, <sup>2</sup>College of Engineering, and <sup>3</sup>Biodynamic Optical Imaging Center, Peking University, Beijing 100871, P. R. China

\* Corresponding author, zhaoxs@pku.edu.cn

### Protein Expression, Purification, and Labeling

Expression, purification, and labeling of the mutants of staphylococcal nuclease (SNase) were performed as described previously.<sup>[1]</sup> Briefly, the K28C/K97C, K97C/K136C, and K28C/H124C mutants were generated by site-directed mutagenesis taking pET-28a-SNase as a template to create functional groups for specific fluorescence labeling. The mutant proteins were reduced with excess of Dithiothreitol (DTT) followed by chromatography in labeling buffer to remove the excess DTT. Site-specific labeling of the reduced mutants was achieved by reaction with thiol-reactive fluorescence dyes Alexa Fluor 546 and Alexa Fluor 647 (Invitrogen). Unconjugated dyes were removed through a PD-10 Desalting Column (GE Healthcare) and the labeled protein solution was stored at -80 °C with 10% glycerol.

### Ensemble CD and Denaturation Measurements

CD spectra were recorded on a Jasco J-815 spectrometer with a band width of 2.00 nm, using a 2 mm path-length cuvette at a scan rate of 50 nm per minute. The protein samples were dissolved in the Tris·HCl buffer of 50 mM Tris·HCl and 100 mM NaCl and the data were corrected for buffer contribution. The K97C/K136C mutant did not significantly deviate from the bands of the CD spectrum of the wild-type SNase (Figure S1).

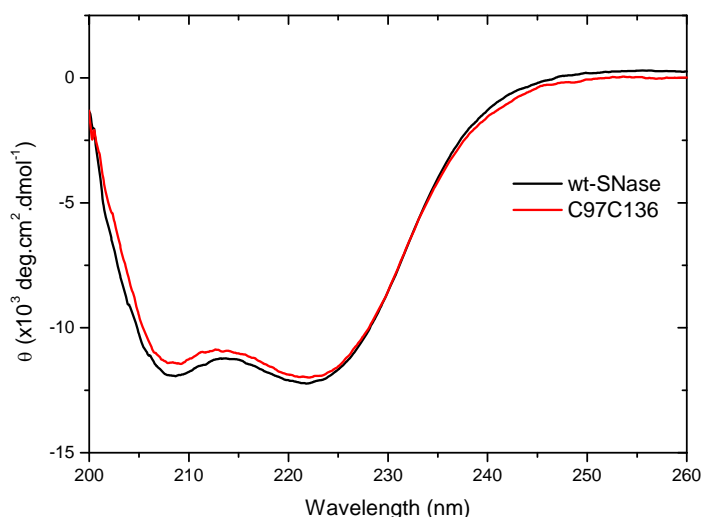


Figure S1. Far-UV CD spectra of the wild-type and K97C/K136C SNase proteins.

The mutagenic K97C/K136C and wild-type proteins at 1  $\mu$ M in Tris·HCl buffer were denatured by various concentrations of GdmCl at 25 °C, and intrinsic Trp140 fluorescence spectra between 305 and 400 nm excited at 295 nm were measured on a Shimadzu RF-5301PC spectrofluorometer. The derived

thermodynamic parameters were shown in Table S1. As in previous case,<sup>[1]</sup> the stability of the mutants was reduced slightly compared to the wild type. The polarizations of the attached donor and acceptor dyes of K97C/K136C in 0-7 M GdmCl solutions were  $0.20 \pm 0.01$  and  $0.15 \pm 0.01$ , respectively, sufficient to use the rotational factor of  $\kappa^2 = 2/3$ .

Table S1. The thermodynamic parameters for the proteins

	$\Delta G^0$ (kcal·mol <sup>-1</sup> )	$m_G$ (kcal·mol <sup>-1</sup> ·M <sup>-1</sup> )	$C_{1/2}$ (M)
wt	6.1	7.3	0.84
K97C/K136C	3.5	6.2	0.56

The CD spectra and the denaturation properties of K28C/K97C and K28C/H124C mutants have already been studied.<sup>[1]</sup>

### **Single Molecule fluorescence Measurements**

Single molecule fluorescence measurements were performed on a home-built dual-channel confocal fluorescence microscope<sup>[1-2]</sup> based on a TE2000 microscope (Nikon). Briefly, the protein sample was excited by a solid-state laser (MLL-III-532, CNI) at 532 nm. The laser power was 130  $\mu$ W in the microfluidic mixer, focused through an oil immersion objective (NA 100  $\times$ , 1.3, Nikon). The donor and acceptor fluorescences were separated from the excitation light by a dichroic mirror (Z532, Chroma) and were spatially filtered using a 30  $\mu$ m pinhole. The passed fluorescences were separated into donor and acceptor components with a second dichroic mirror (FF650-Di01, Semrock) and two final filters (FF01-593/40 and FF01-692/40, Semrock for the donor and acceptor channels, respectively). Each component was detected by a photon-counting avalanche photodiode (APD) (SPCM-AQRH-14, Perkin-Elmer Optoelectronics). Fluorescence intensities were recorded with a photon counters card (PMS-400A, Becker & Hickl). The smFRET time traces and the autocorrelation FCS curves were simultaneously recorded using a multiple-digital hardware correlator device (Flex02- 01D, www.correlator.com).

### **Microfluidic Mixing Device**

The construction of the microfluidic mixer has been reported previously.<sup>[3]</sup> Briefly, it was consisted of a PDMS (RTV 615, GE Silicones) chip sealed by a No.1 coverglass (Fisher Scientific). The microfluidic channels were specially designed for the smFRET measurement. The PDMS chip was a cast of a master mold fabricated in a UV lithography process, spinning a 20  $\mu$ m layer of an epoxy negative photoresist SU8 2010 (MicroChem) onto a 3 inch silicon wafer, curing on a hot plate and developing. Before casting, the wafer was silanized with the vapor of TMCS for 15 min to prevent PDMS adhesion. The mixture of RTV 615 A+B kit was poured onto the master mold and baked at 80 °C for 8 h. The PDMS chip was peeled off the wafer and punched to make inlet and outlet holes. A permanent PDMS-coverglass device was made using an air plasma, the coverglass was cleaned in a piranha solution previously.

The protein sample and buffer were delivered into the inlets from two reservoirs of 0.6 mL centrifugetubes, which were connected to compressed air. The pressure of compressed air was regulated by two precise pressure regulators (8286AMBF2.5, Porter Instruments) and measured with a accuracy digital pressure gauge (DPG4000-30, Omega). The resolution of the regulators was 0.01 kPa with a careful tuning. A high pressure regulator at 150 kPa was used to drive the solutions into the mixer to focus the sample stream in a short time before data acquisition. After forming a stable focused stream, the pressures of the reservoirs were switched for single-molecule experiments. The microfluidic chip was holded in an adaptor made of aluminum and transparent plastic to fix the chip on the microscope stably (Figure S2).

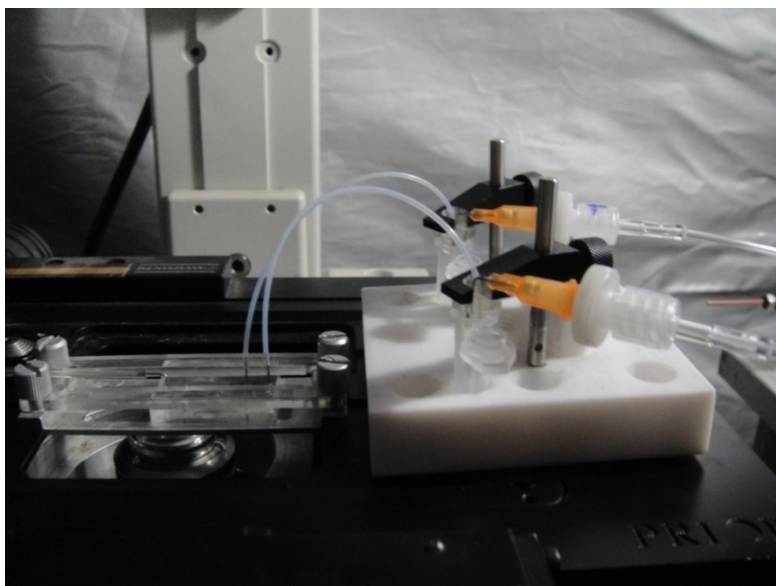


Figure S2. The setup of microfluidic mixer. The chip was fixed in an adaptor made of aluminum and transparent plastic stably. The protein sample and buffer were filled in 0.6 mL centrifuge tubes, delivered into the chip inlets by compressed air regulated by two pressure regulators.

### **Denaturant Concentration in The Detection channel**

The final denaturant concentration in the detection channel was determined by comparing the FRET efficiency of the unfolded state with that in equilibrium experiments. The FRET efficiency histograms were fitted using lognormal and Gaussian functions, the unfolded state with Gaussian function and the native state with lognormal function. In single-molecule mixing experiments, the mean FRET efficiencies of the unfolded state of the mutant K97C/K136C after reaching the equilibrium was measured to be  $0.835 \pm 0.004$ . We measured the mean FRET efficiencies of the unfolded state of the mutant K97C/K136C in equilibrium at different denaturant concentrations using the method described previously.<sup>[1]</sup> Figure S3 shows the dependence of the apparent mean FRET efficiencies of the unfolded state on the GdmCl concentration in static experiments. By interpolation, we found that the GdmCl concentration in the detection channel was 0.49 M.

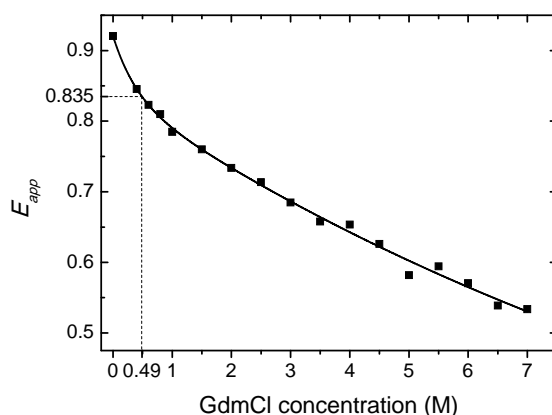


Figure S3. Dependence of the apparent mean FRET efficiencies of the unfolded state on the GdmCl concentration. The final GdmCl concentration in the single-molecule mixing was determined to be 0.49 M by interpolation.

### **Measurements on flow velocity using FCS**



The flow velocity in the channels were measured by FCS simultaneously with the smFRET data acquisition.<sup>[3]</sup> The radius of the focus volume was determined to be  $r_0 = 270 \pm 7$  nm using the sample of Rhodamine 6G. In the mixing experiments, autocorrelation FCS curves of the donor channel were fitted using a model considering diffusion, flow velocity, and reactions.<sup>[3]</sup>

The flow velocity was regulated to be around  $1 \text{ mm}\cdot\text{s}^{-1}$  in the detection channel to achieve a high signal to noise ratio, with the side inlet pressure at 6.0 kPa and the centre inlet pressure at 7.8 kPa. The pressures would vary slightly among different mixers due to slight variation in the fabrication. The position of the detection point in the detection channel was converted to the reaction time using the measured flow velocity.

### A double-exponential curve is needed for the whole protein molecule

Figure S4 shows the fitting results using single-exponential and double-exponential kinetic models of the mutant K28C/H124C corresponding to the whole protein molecule. In the main panel, the lines show the fittings to the folding data, using nonlinear least-squares analysis. In the panel below, the corresponding residuals are compared with both models. The results show that inclusion of two exponential terms was indeed necessary.

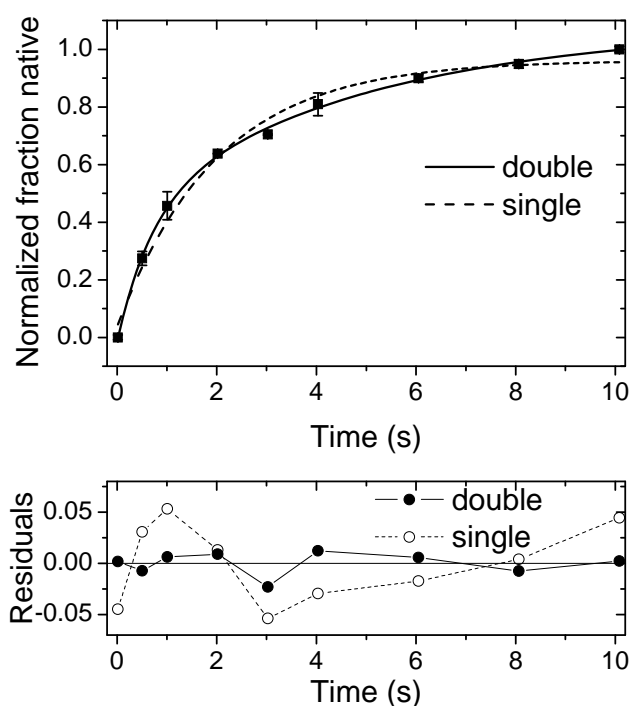


Figure S4. Comparison of single-exponential and double-exponential models. From both the fitted curves and residuals, the double-exponential model fits the folding data better.

- [1] P. C. Liu, X. L. Meng, P. Qu, X. S. Zhao, C. C. Wang, *J. Phys. Chem. B* **2009**, *113*, 12030-12036.
- [2] X. D. Chen, Y. Zhou, P. Qu, X. S. Zhao, *J. Am. Chem. Soc.* **2008**, *130*, 16947-16952.
- [3] Z. Zhi, P. Liu, Y. Huang, X. S. Zhao, *Acta. Phys. Chim. Sin.* **2011**, *27*, 1990-1995.